

Renovation of the IPM-2 source ion-optical system for the Globus-M2 spherical tokamak neutral beam injector

© A.Yu. Telnova,¹ V.B. Minaev,¹ A.A. Panasenkov,² P.B. Shchegolev¹

¹ Ioffe Institute, St. Petersburg, Russia

² National Research Center „Kurchatov Institute“, Moscow, Russia

e-mail: anna.telnova@mail.ioffe.ru

Received November 12, 2021

Revised December 23, 2021

Accepted December 24, 2021

The paper is devoted to the IPM-2 ion source ion-optical system preparation for the plasma heating experiments with a neutral beam in the Globus-M2 spherical tokamak. Within the framework of this work, a complete renovation of the ion-optical system of the ion source was carried out, including its assembly, adjustment, and testing. To assess the quality of the work performed, measurements were made of the main electrical parameters of the high-energy beam, its energy spectrum and signals from secondary emission probes. Based on the data obtained, the beam power distribution profile and its characteristic dimensions are reconstructed, and the relative concentrations of the energy components of the beam are calculated.

Keywords: nuclear fusion, neutral beam injection, neutral beam injector, ion source.

DOI: 10.21883/TP.2022.04.53600.292-21

Introduction

The NI-1 atomic injector [2], which was constructed in the 1970s at the Kurchatov Institute for the T-11 tokamak, is used in experiments at the Globus-M spherical tokamak [1] as the primary instrument for plasma heating. Globus-M2 is a new compact spherical tokamak [3,4] that is the upgraded version of Globus-M (with aspect ratio $A = 1.5$, major radius $R = 0.36$ m, and minor radius $a = 0.24$ m). Toroidal magnetic field B_T and plasma current I_p may be increased in the new setup to 1 T and 500 kA, respectively. The diagnostic complex [5] and the neutral injection complex, which was fitted with the second injector (NI-2) [6], were upgraded in the transition to Globus-M2.

The NI-1 injector supports injection of a hydrogen or deuterium beam with a particle energy up to 30 keV and a duration up to 50 ms. The maximum power of a neutral beam at the injector outlet is 0.5 or 1.0 MW depending on the type of ion source installed (IPM-2 or IPM-1). The present study is focused on renovation of the ion-optical system of the IPM-2 source, analysis of the quality of executed works, and preparation of the source to experiments on additional plasma heating at the Globus-M2 spherical tokamak. This paper contains a great number of technical terms related to the physics of ion sources and atomic beams; in order to gain a deeper understanding of this field, the reader may consult specialized literature [7-10].

1. Adjustment of the ion-optical system of the IPM-2 source

1.1. Design of the ion-optical system

The multi-slit ion-optical system (IOS) consisting of three electrodes (emission electrode (EE), negative electrode (NE), and grounded electrode (GE)) is used to form and extract an ion beam in an IPM-type source (source with a peripheral magnetic field). The electrical field generated in the accelerating gap forms a plasma emitter at the slits of EE lenses and extracts an ion flux. The NE provides overall beam focusing and blocks the back flow of secondary plasma electrons. The GE ensures that the emerging ion beam has „zero“ potential. Figure 1 shows the assembled NE lens of the IPM-2 source and replacement grids for it.

The IOS of the source ensures overall beam focusing in two directions: horizontal (due to the fact that EE and NE grids are curved along slits with a curvature radius on the order of 2.5 m) and vertical (due to the fact that the outermost NE grids (the bottom and the top one in Fig. 1) are shifted apart in the vertical direction relative to the corresponding EE grids).

According to the design of the IPM-2 ion source, the shift of the outermost NE grids relative to the center axis should be $\Delta y = 200 \mu\text{m}$. This corresponds to a focal distance of 2.5 m.

With zero shift, the configuration of equipotential lines in the NE slit region forms a diverging lens with focal distance $F \approx 1.6d$, where d is the EE-NE gap [7,8] (Fig. 2) [9]. It should be noted that a certain effective value d_{eff} , which is



Figure 1. Assembled NE lens of the IPM-2 source and replacement grids for it.

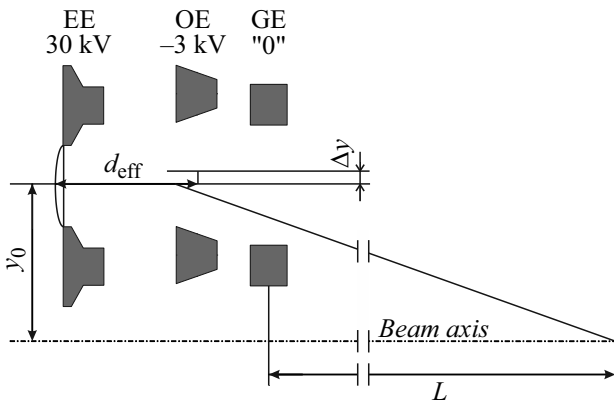


Figure 2. Geometry of the slit cell of the IPM source IOS and beam focusing in the direction perpendicular to the slits performed by shifting the NE relative to the EE.

greater than the actual interelectrode distance, is taken as d , since it accounts both for the EE thickness and the „sag“ of the electric field in the NE lens slit. The effective size of the accelerating gap is $d_{\text{eff}} = t_1 + d + \delta_2$, where t_1 is the EE thickness and δ_2 is the half-width of the NE slit aperture. It can be said that, to a sufficient degree of approximation, each cell operates independently, and the beam as a whole is a combination of individual elementary beams. The angle of inclination of their axes defines the beam focusing in the vertical direction (across the slits). In order for an elementary beam emerging from a certain EE slit located at distance y_0 from the central slit (through which the beam axis goes) to cross the beam axis at point located at

distance L from the source, the NE slit center needs to be positioned at distance $y_0 + \Delta y$ from the beam axis, where shift Δy is determined using relation $y_0/L = 0.625\Delta y/d_{\text{eff}}$: $\Delta y = 1.6d_{\text{eff}} : y_0/L$. The overall beam size is defined by the angular divergence of elementary beams and distance L . The constraint on the beam size is imposed by dimensions of the tokamak inlet (26.5×8.5 cm).

1.2. IPM-2 IOS assembly

The key design parameters of the IPM-2 source are listed in Table 1.

Following the IPM-1 source accident, the IPM-2 source was installed at the injector. The signals from secondary emission probes, which were installed at the beam receiver [2], during an injector shot revealed a considerable increase in the vertical beam size. This is indicative of focusing issues in the IOS. It should be noted that maintaining the design accuracy of alignment of grids at the IOS electrodes is one of the key issues in assembly and adjustment of a multi-slit IOS. The permissible grid fabrication error is $\pm 20 \mu\text{m}$. An IZA-2 linear comparator [11], which is designed for length measurement with an accuracy up to $1 \mu\text{m}$, was used to verify the quality of fabrication of grids and for IOS adjustment. As was already noted, the IOS of the IPM-2 ion source consists of three lenses (electrodes) with three grids of 14 slits in each of them (42 elementary cells in total; see Fig. 1).

The EE, NE, and GE lenses were measured first, and the shift of NE slits relative to the EE was determined based on the obtained data. It turned out that the linear sizes of certain elementary cells and the overall shifts of the outermost NE grids relative to the EE changed in the course of operation. This is illustrated by Fig. 3, where the shifts of centers of NE slits relative to the centers of EE slits for each elementary cell are indicated. The obtained

Table 1. Key parameters of the IPM-2 source

Maximum ion beam power, MW	hydrogen	1.0
	deuterium	0.7
Maximum accelerating voltage, kV		30
Maximum current of the hydrogen ion beam, A		35
Maximum current of the deuterium ion beam, A		25
Number of grids in electrodes		3
Focal distance, m	— in the horizontal plane	2.5
	— in the vertical plane	2.5
Beam divergence angle, degrees:	— horizontal (along slits)	± 0.6
	— vertical (across slits)	± 1.5
Percentage of components $\text{H}_1^+/\text{H}_2^+/\text{H}_3^+$ (at a current density of 0.4 A/cm^2), %		75/18/7

data suggest that the shifts of both top and bottom grids differ considerably from the design values (approximately $100\ \mu\text{m}$ for the bottom grid and $250\ \mu\text{m}$ for the top one). An upward shift in excess of $250\ \mu\text{m}$ is unacceptable, since it has a negative effect on the transparency of the optical system as a whole and increases the risk of an elementary beam falling directly onto a structural element of the NE grid. The focal distances for each elementary cell of the IOS were calculated based on the measurement data for grids and estimates of their relative shifts. The results of calculations revealed a significant deterioration of IOS focusing performance due to unbalanced heat loads imposed on electrodes (breakdowns, local overheating, etc.) in the process of operation of the source. These heat inputs inevitably alter the IOS lens geometry (not least because of the deformation of structural grid elements that form slit apertures).

The measurement results indicate that the IPM-2 source requires renovation: certain IOs grids need to be replaced, and the system as a whole needs to be reassembled, adjusted, and aligned. It was decided after a thorough inspection and analysis that the current EE grids may remain in place, but the entire set of damaged NE and GE grids should be replaced. The optimum fitting of individual EE and NE grids was chosen in the following way.

1. All EE and NE grids were measured to estimate the quality of their fabrication. The grids were then compared based on the obtained measurement data in order to determine the best pairwise matches between different electrodes.

2. The grids were arranged on electrode lenses to set the predetermined shift of the outermost NE grids.

The optimum mutual arrangement of grids in lens assemblies providing the needed beam focusing was chosen as a result.

The measured shifts for the new IOS assembly are presented in Fig. 3 (crosses): the needed EE–NE alignment

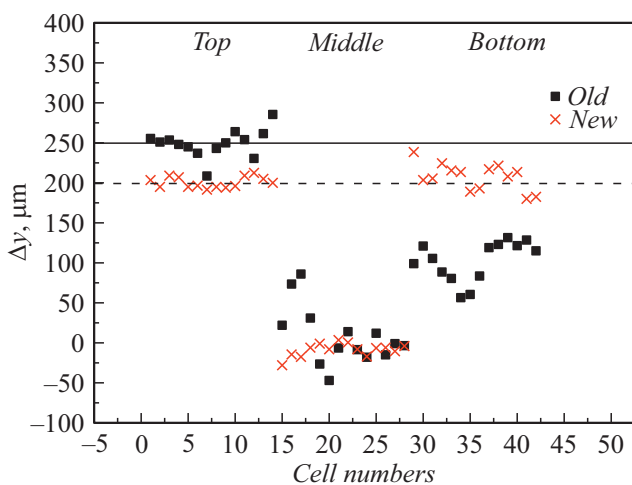


Figure 3. Shifts (measured from the beam axis) of the centers of NE slits relative to the centers of EE slits in the old and new IPM-2 IOS.

Table 2. Operating parameters of the injector in the course of verification of the IOS assembly quality

EE voltage, kV	26
EE current, A	19–24
Pulse duration, ms	40
Working gas	deuterium

accuracy was achieved, the focal distance is approximately equal to $2.5\ \mu\text{m}$, and the shift of NE grids does not exceed $250\ \mu\text{m}$. The measurements of GE grids revealed that their segments were deformed and could affect the IOS transparency. Therefore, they were replaced. The direct influence of the GE lens on focusing is insignificant, but its segments should not interfere with the beam propagation.

2. Tests of the IPM-2 source and estimation of the quality of IOS renovation

In order to test IPM-2 and verify the focusing quality of the updated IOS, the ion source was installed at the injector, where it was subjected to vacuum tests and high-voltage aging. This procedure is performed to clean the surfaces of IOS electrodes with repeated high-voltage breakdowns of a limited energy. When all tests and the injector ramp-up sequence were completed, the quality of IOS assembly was checked by finding the optimum EE current at a fixed accelerating voltage with the beam size being monitored (data from secondary emission probes at the beam receiver were used). The operating parameters of the injector in the course of verification of the IOS assembly quality are listed in Table 2.

With the optimum EE current, the beam has the best focusing across the IOS slits (and, consequently, the smallest size); in the contrary case, it spreads out in the vertical direction. The focusing performance was assessed based on the profile of power density of an atomic beam reconstructed from signals of 22 secondary emission probes of the beam receiver. The reconstruction procedure, which was detailed in [2], allows one to restore the profile of distribution of the power density over the beam section and thus estimate the quality of focusing. The DAS Tools code [12] was used to visualize and analyze the probe measurement data. In order to estimate the quality of focusing, the values of beam height ΔY [cm] at a power density level of $1/e$ were compared at different EE currents. The results of this comparison are presented in Fig. 4.

The minimum of the obtained saddle-type dependence was at a current of 21.5–22 A, which is the optimum one for an accelerating voltage of 26 kV. The corresponding vertical beam size at a level of $1/e$ is 11.5–12 cm, which

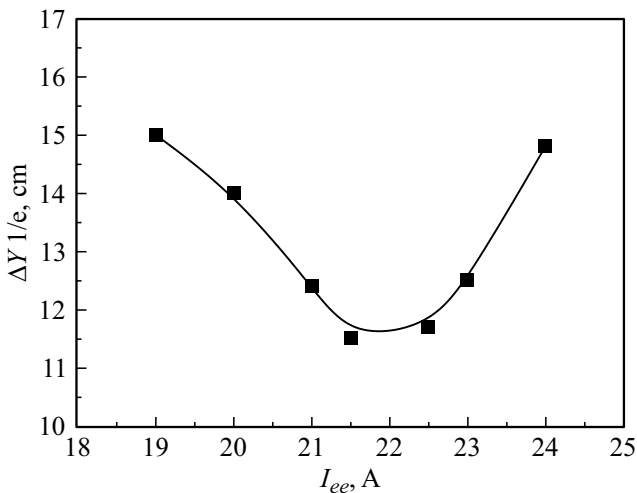


Figure 4. Dependence of the beam height at a level of 1/e on the EE current at a fixed accelerating voltage of 26 kV.

translates into 16–17 cm at a power density level of 0.9 and is indicative of tight focusing.

It now becomes possible to estimate the power of ion and atomic beams at the optimum current of the emission electrode. We use the formulae from [2] to do this. The coefficients of conversion of an ion beam into an atomic one and transport coefficient $\eta_{io} \times \eta_{tr}$ may be estimated based on the ratio of signals of identical probes with the electromagnet being switched on and off. The power of a deuterium beam determined in this way at an energy of 26 keV is 400 kW.

In order to assess the quality of IOS renovation, the size of the beam obtained using the updated IOS was compared to the sizes of beams produced in earlier experimental campaigns of the IPM-2 source with a different IOS assembly at the optimum beam parameters and an accelerating voltage of 26 kV. The discharge parameters are listed in Table 3. Discharge No. 407815 belongs to the series of experiments with the new IOS assembly. The NE voltage in these discharges was 3 kV, and the NE current was 1.5 A.

Figure 5 presents the oscilloscope records of the key signals for the corresponding discharges for a beam with an energy of 26 keV.

The results of reconstruction of the width and the height of beams for the considered discharges are presented in Figs. 6 and 7, respectively.

Table 3. Key parameters of discharges from different IPM-2 series

N NBI	U_{ee} , kV	I_{ee} , A	t , ms	Gas
318961	26	20.7	40	D
318962	26	22.7	40	D
321256	26	23.5	40	D
407815	26	22	40	D

Figure 5 demonstrates that the beam width in the new IOS assembly increases almost by a factor of 2. This is the result of installation of a new set of NE grids without shaping (i.e., the curvature radius is zero). The height of beams in different IOS assemblies remains almost unchanged. This is indicative of fine focusing in the vertical direction.

Thus, the size of the IPM-2 beam after renovation at the receiver is $X \times Y = 5 \times 13$ cm at a power density level of 1/e, and the horizontal beam size does not exceed 8 cm, which is less than the width of the interface connector of the injector (8.5 cm).

3. Preparation of a neutral beam for experiments at the Globus-M2 spherical tokamak

A deuterium beam with the maximum possible energy and power needs to be injected in experiments at the

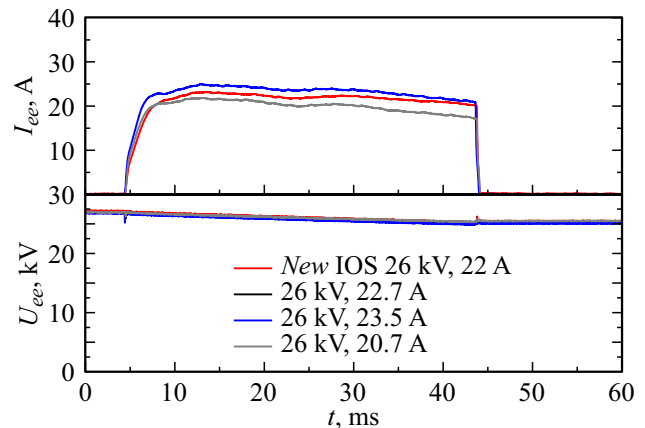


Figure 5. Oscilloscope records of the key signals for discharges from Table 3: EE current and EE voltage.

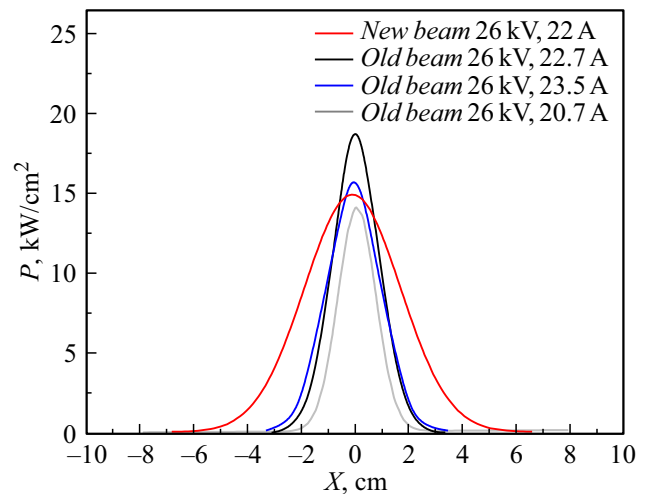


Figure 6. Profile of the distribution of the power density of beams with width.

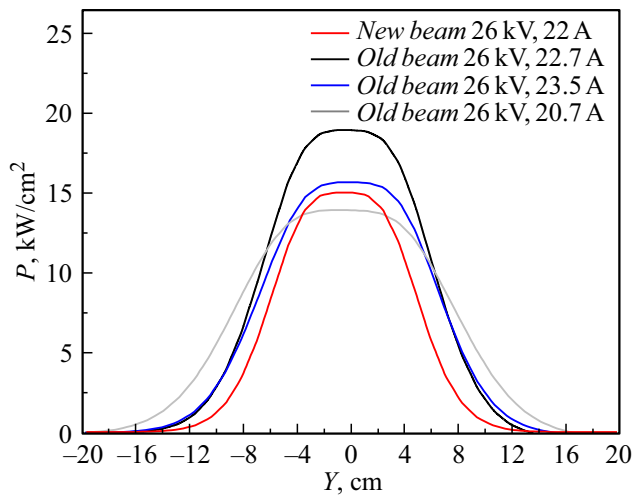


Figure 7. Profile of the distribution of the power density of beams with height.

Globus-M2 spherical tokamak to maximize the neutron yield in discharges with additional plasma heating. According to the design parameters (Table 1) of the IPM-2 source, the maximum power of a deuterium ion beam is as high as 0.7 MW at an energy of 30 kV. Beam parameters close to these ones were obtained by increasing gradually the EE voltage (U_{ee}) and raising its current (I_{ee}) proportionally (Fig. 8).

The optimum EE current for deuterium corresponding to the maximum design EE voltage for the IPM-2 source (30 kV) was 25 A. The ion beam power was estimated as $P_i = U_{ee} \cdot (I_{ee} - (1/2)I_{oe})$, where I_{oe} is the negative electrode current. This formula yields time-average power P_i of approximately 700 kW. The accelerating voltage decreases slightly within the injection pulse due to discharge of the supply storage capacitor. In addition, the gas discharge in the source is not entirely steady-state: although the discharge current remains constant, the discharge voltage varies considerably within the injection time. These two factors exert a combined influence on the shape of the extracted ion current pulse and, consequently, on focusing. However, since the beam size across the grids varies only slightly with time, the beam focusing may be considered adequate throughout the entire injection pulse. This is confirmed by the temporal evolution of the beam height at a power density level of $1/e$ (Fig. 7). The resulting average total power of an atomic beam injected into the tokamak is 500 kW, and its variations do not exceed 10%.

The key parameter of a beam injected into the tokamak is its energy composition (the percentage ratio of beam components with different energy at the neutralizer output). In addition to atomic ions D_1^+ , an ion beam ejected from the source contains a certain amount of molecular ions D_2^+ and D_3^+ and impurity hydroxyl ions D_2O^+ , which are introduced into the beam as a result of specific processes occurring in arc-discharge plasma in the gas-discharge

chamber. Passing through the charge-exchange target in the neutralizer, molecular ions capture an electron and dissociate into atoms with energies E , $E/2$, $E/3$ (E is the main energy) from fast ions D_1^+ , D_2^+ , D_3^+ , respectively, while hydroxyl ions D_2O^+ dissociate into atoms with energy $E/10$. Charged particles are removed from the beam by a magnetic field at the neutralizer output. The remaining atoms are excited in collisions with background gas and emit the D_a line. The energy distribution of beam particles is determined using a noncontact diagnostic method (see its detailed description in [13]) based on the detection of emission with a wavelength shifted due to the Doppler effect. Owing to the Doppler shift, groups of atoms emit spectral lines of separate wavelengths corresponding to the particles with energy E , $E/2$, $E/3$, and $E/10$. The detection of emission produced in interaction between the beam and residual gas allows one to identify these spectral lines. An example spectrum of this kind for the atomic beam with the maximum power, the principal oscilloscope records of which are shown in Fig. 8, is presented in Fig. 9.

Five lines are discernible: one intense line on the left corresponds to the emission of atomic deuterium upon excitation of background gas by the beam (line D_a), and three strongly shifted lines on the right correspond to fast atoms with energies E , $E/2$, $E/3$. The line closest to the unshifted one represents the emission of deuterium atoms $E/10$. The spectrum for the deuterium beam also contains a small peak to the right of the line corresponding to atoms with energy E . This peak is indicative of the presence of impurity hydrogen in deuterium. Having analyzed the obtained spectrum of the deuterium beam, we determined the relative concentrations of atoms with energy E (59%), $E/2$ (19%), $E/3$ (6%), and $E/10$ (16%). If we exclude the component associated with hydroxyl ions,

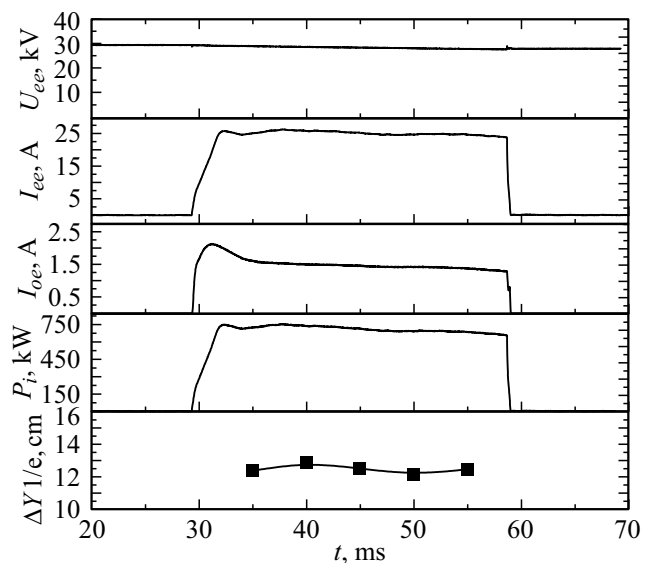


Figure 8. Temporal dependences of the EE voltage, EE current, NE current, ion beam power, and beam height at a power density level of $1/e$.

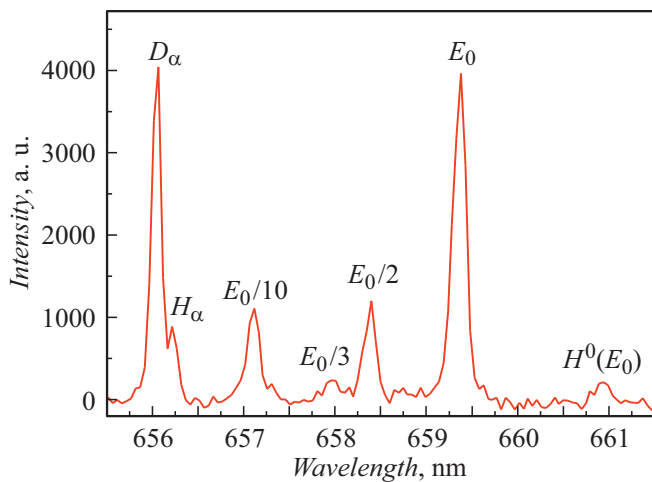


Figure 9. Emission spectrum of a deuterium beam injected into the tokamak plasma.

the ratio of components of a „pure“ beam is E — 70%, $E/2$ — 23%, $E/3$ — 7%. Converting these results into fractions of power carried by different components, we find that the bulk of beam power ($\sim 70\%$) corresponds to atoms with energy E , while the power attributable to particles with energy $E/10$ is negligible (less than 1%).

Conclusion

The IPM-2 ion source was renovated in the process of preparation of the neutral injection complex to experiments on plasma heating and current generation at the Globus-M2 spherical tokamak. The initial assessment of the IOS focusing revealed that the focal distance is not consistent with the design requirements, and a new IOS was assembled and adjusted. Following the installation of IPM-2 at the injector, the optimum EE current corresponding to the best beam focusing across the IOS slits was determined for the chosen EE voltage, and the quality of focusing was compared to that from earlier IPM-2 experimental campaigns. It was confirmed as a result that the vertical focusing in the source is adequate and agrees closely with the design parameters. However, since the new set of NE grids were not shaped, the quality of horizontal beam focusing decreased, and the new beam size was $X \times Y = 5 \times 13$ cm at a power density level of $1/e$. In addition, the maximum design parameters for a deuterium beam were achieved once again at the source, and the total injected power was 500 kW. Thus, the renovation and high-voltage aging of IMP-2 make it possible to perform experiments on neutral injection at the Globus-M2 spherical tokamak.

Acknowledgments

The key beam parameters were measured at the unique scientific complex Globus-M Spherical Tokamak, which is a

part of the federal common research center Material Science and Diagnostics in Advanced Technologies.

Funding

The studies reported in Section 1 were supported by the Ioffe Institute under state assignment 0040-2019-0023. The studies reported in Section 2 were supported by the Russian Science Foundation, project No. 17-72-20076. The studies reported in Section 3 were performed under state assignment 0034-2021-0001.

Conflict of interest

The authors declare that they have no conflict of interest.

References

- [1] V.K. Gusev, V.E. Golant, E.Z. Gusakov, V.V. D'yachenko, M.A. Irzak, V.B. Minaev, E.E. Mukhin, A.N. Novokhatskii, K.A. Podushnikova, G.T. Razdobarin, N.V. Sakharov, E.N. Tregubova, V.S. Uzlov, O.N. Shcherbinin, V.A. Belyakov, A.A. Kavin, Yu.A. Kostsov, E.G. Kuz'min, V.F. Soikin, E.A. Kuznetsov, V.A. Yagnov. *Tech. Phys.*, **44** (9), 1054 (1999). DOI: 10.1134/1.1259469
- [2] V.K. Gusev, A.V. Dech, L.A. Esipov, V.B. Minaev, A.G. Barsukov, G.B. Igon'kina, V.V. Kuznetsov, A.A. Panasenkov, M.M. Sokolov, G.N. Tilinin, A.V. Lupin, V.K. Markov. *Tech. Phys.*, **52** (9), 1127 (2007). DOI: 10.1134/S1063784207090058
- [3] V.B. Minaev, V.K. Gusev, N.V. Sakharov, V.I. Varfolomeev, N.N. Bakharev, V.A. Belyakov, E.N. Bondarchuk, P.N. Brunkov, F.V. Chernyshev, V.I. Davydenko, V.V. Dyachenko, A.A. Kavin, S.A. Khitrov, N.A. Khromov, E.O. Kiselev. *Nucl. Fusion*, **57**, 066047 (2017). DOI: 10.1088/1741-4326/aa69e0
- [4] V.K. Gusev, N.N. Bakharev, V.A. Belyakov, B.Ya. Ber, E.N. Bondarchuk, V.V. Bulanin, A.S. Bykov, F.V. Chernyshev, E.V. Demina, V.V. Dyachenko, P.R. Goncharov, A.E. Gorodetsky, E.Z. Gusakov, A.D. Ibyaminova, A.A. Ivanov. *Nucl. Fusion*, **55**, 104016 (2015). DOI: 10.1088/0029-5515/55/10/104016
- [5] N.N. Bakharev, I.M. Balachenkov, F.V. Chernyshev, I.N. Chugunov, V.V. Dyachenko, V.K. Gusev, M.V. Iliasova, E.M. Khilkevitch, N.A. Khromov, E.O. Kiselev, A.N. Konovalov, G.S. Kurskiev, V.B. Minaev, A.D. Melnik, I.V. Miroshnikov, A.N. Novokhatsky, M.I. Patrov, Yu.V. Petrov, N.V. Sakharov, P.B. Shchegolev, A.E. Shevelev, O.M. Skrekel, A.Yu. Telnova, V.A. Tokarev, S.Yu. Tolstyakov, E.A. Tukhmenova, V.I. Varfolomeev, A.V. Voronin. *Plasma Phys. Reports*, **46** (7), 675 (2020). DOI: 10.1134/S1063780X20070016
- [6] A.Y. Telnova, V.B. Minaev, P.B. Shchegolev, N.N. Bakharev, I.V. Shikhovtsev, V.I. Varfolomeev. *J. Phys.: Conf. Ser.*, **1400**, 077015 (2019). DOI: 10.1088/1742-6596/1400/7/077015
- [7] N.N. Semashko, A.N. Vladimirov, V.V. Kuznetsov, V.M. Kulygin, A.A. Panasenkov. *Inzhektory bystrykh atomov vodoroda* (Energoizdat, M., 1981), 168 pp (in Russian).

- [8] M.D. Gabovich, N.V. Pleshivtsev, N.N. Semashko. *Puchki ionov i atomov dlya upravlyaemogo termoyadernogo sinteza i tekhnologicheskikh tselei* (Energoatomizdat, M., 1986), 249 pp (in Russian).
- [9] A.G. Barsukov. Candidate's Dissertation in Engineering (NRC Kurchatov Institute, M., 2005) (in Russian).
- [10] I.G. Brown (Ed.) *The Physics and Technology of Ion Source* (Wiley, NY., 1989)
- [11] G.I. Fedotov, R.S. Il'in, L.A. Novitskii, G.E. Zubarev, A.S. Gomenyuk. *Laboratornye opticheskie pribory: uchebnoe posobie dlya priborostroitel'nykh i mashinostroitel'nykh vuzov* (Mashinostroenie, M., 1979), 2nd ed. (in Russian).
- [12] G.B. Igon'kina, M.M. Sokolov, G.N. Tilinin. Proc. 11th National Russian Conf. on Plasma Diagnostics (Troitsk, 2005) (in Russian).
- [13] P.B. Shchegolev, V.B. Minaev, I.V. Miroshnikov. Nauchno-Tekh. Vedomosti SPbGPU. Fiz.-Mat. Nauki, **4**, 79 (2012) (in Russian).